

# A NOTCH3-CXCL12-driven myeloma-tumor niche signaling axis promotes chemoresistance in multiple myeloma

Hayley M. Sabol,<sup>1</sup> Cody Ashby,<sup>2,3</sup> Manish Adhikari,<sup>1</sup> Aric Anloague,<sup>1</sup> Japneet Kaur,<sup>1</sup> Sharmin Khan,<sup>1</sup> Samrat Roy Choudhury,<sup>3,4</sup> Carolina Schinke,<sup>3,5</sup> Michela Palmieri,<sup>6</sup> C. Lowry Barnes,<sup>7</sup> Elena Ambrogini,<sup>6</sup> Intawat Nookaew<sup>2,3</sup> and Jesus Delgado-Calle<sup>1,3</sup>

<sup>1</sup>Physiology and Cell Biology, University of Arkansas for Medical Sciences; <sup>2</sup>Department of Biomedical Informatics, University of Arkansas for Medical Sciences; <sup>3</sup>Winthrop P. Rockefeller Cancer Institute, University of Arkansas for Medical Sciences; <sup>4</sup>Pediatric Hematology-Oncology, Arkansas Children's Research Institute, University of Arkansas for Medical Sciences; <sup>5</sup>Myeloma Center, University of Arkansas for Medical Sciences; <sup>6</sup>Division of Endocrinology and Metabolism, Center for Osteoporosis and Metabolic Bone Diseases and Center for Musculoskeletal Disease Research, University of Arkansas for Medical Sciences and Central Arkansas Veterans Healthcare System and <sup>7</sup>Department of Orthopedic Surgery, University of Arkansas for Medical Sciences, Little Rock, AR, USA

**Correspondence:** J. Delgado-Calle  
[jdelgadocalle@uams.edu](mailto:jdelgadocalle@uams.edu)

**Received:** October 10, 2023.

**Accepted:** February 13, 2024.

**Early view:** February 22, 2024.

<https://doi.org/10.3324/haematol.2023.284443>

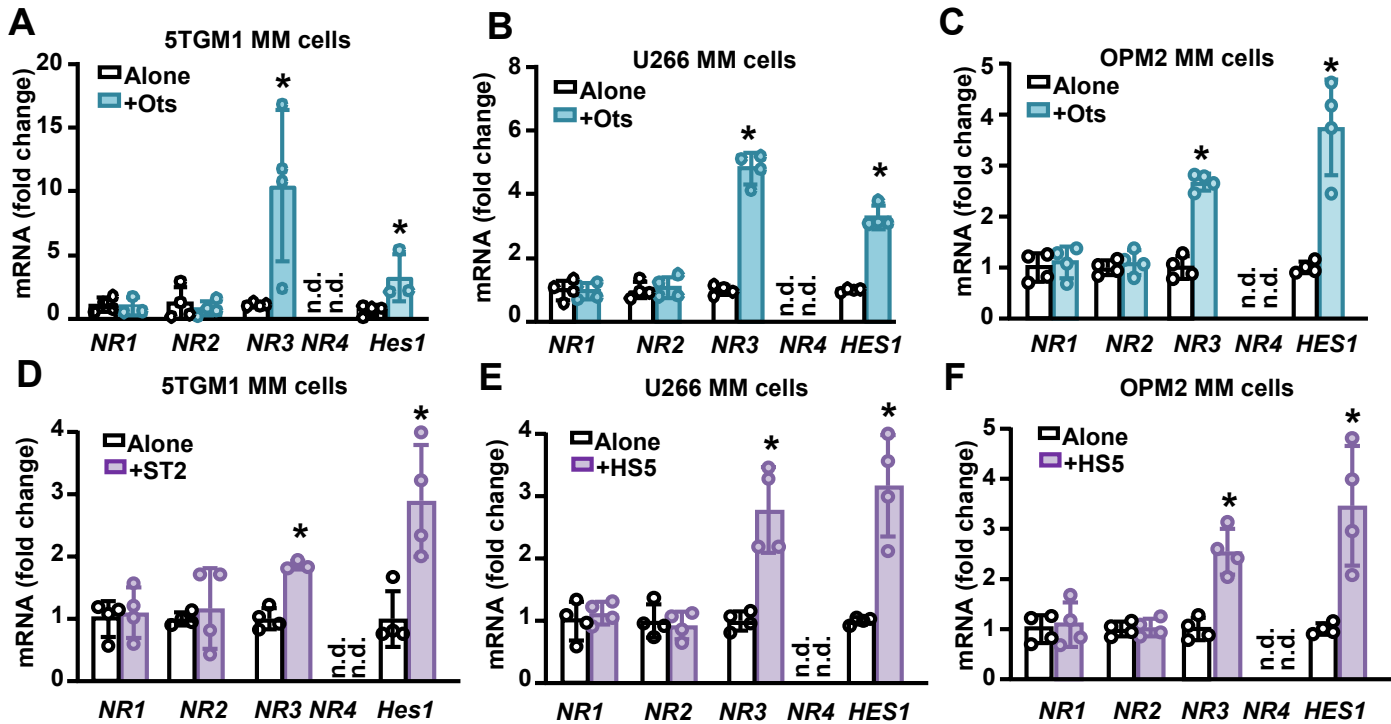
©2024 Ferrata Storti Foundation

Published under a CC BY-NC license

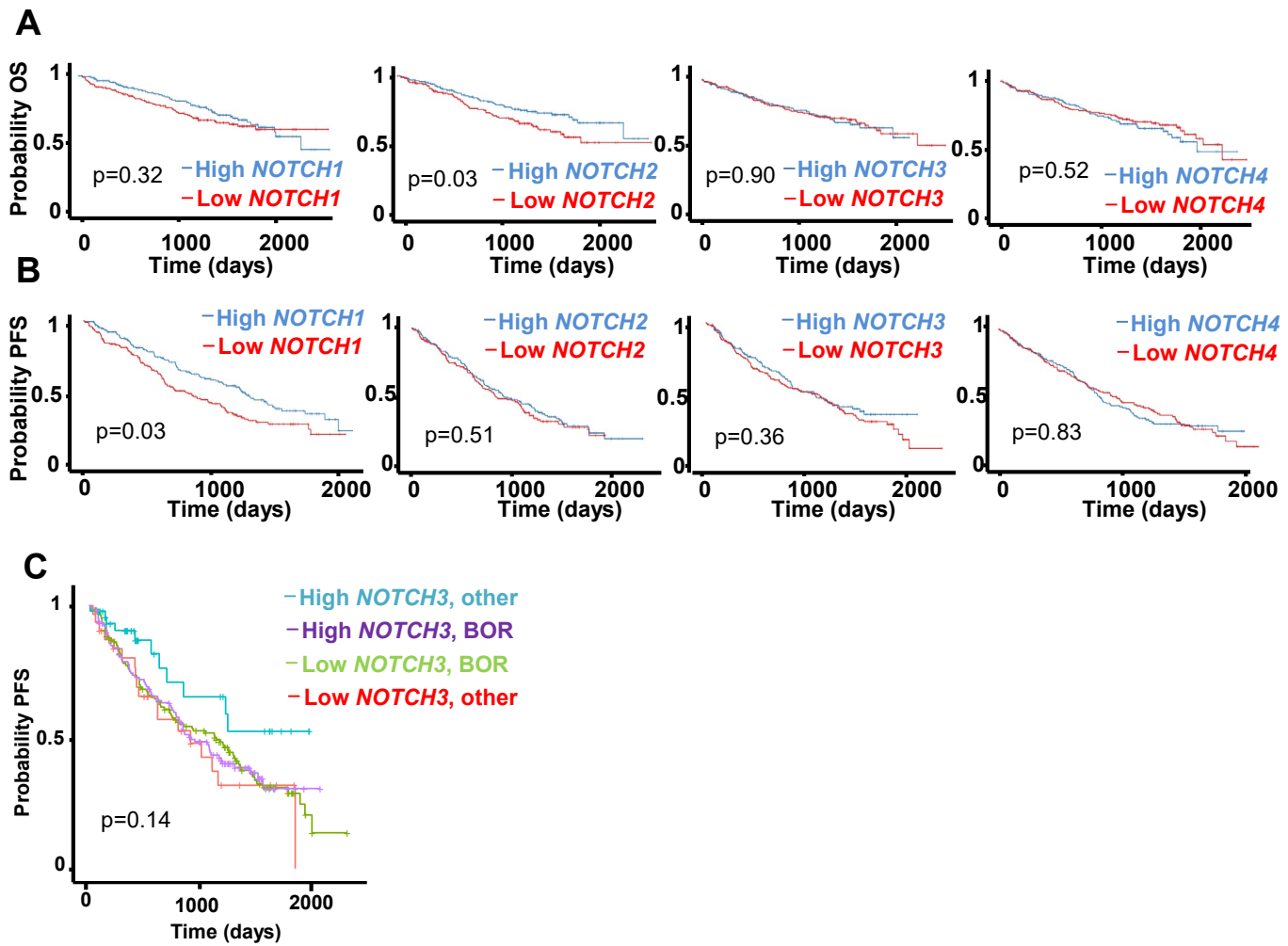


Chr	Position	Ref	Alt	Sample
19	15276696	G	A	MMRF_1037_1_BM
19	15299048	G	A	MMRF_1078_1_BM
19	15272330	G	A	MMRF_1290_1_BM
19	15278081	C	T	MMRF_1401_1_BM
19	15303250	C	T	MMRF_1689_1_BM
19	15272059	T	C	MMRF_1755_1_BM
19	15299116	C	G	MMRF_1796_1_BM
19	15281535	G	A	MMRF_1981_1_BM
19	15291836	C	T	MMRF_2314_1_BM
19	15281260	G	A	MMRF_2723_1_BM
19	15284979	G	A	MMRF_2834_1_BM
19	15291067	C	G	MMRF_2843_1_BM

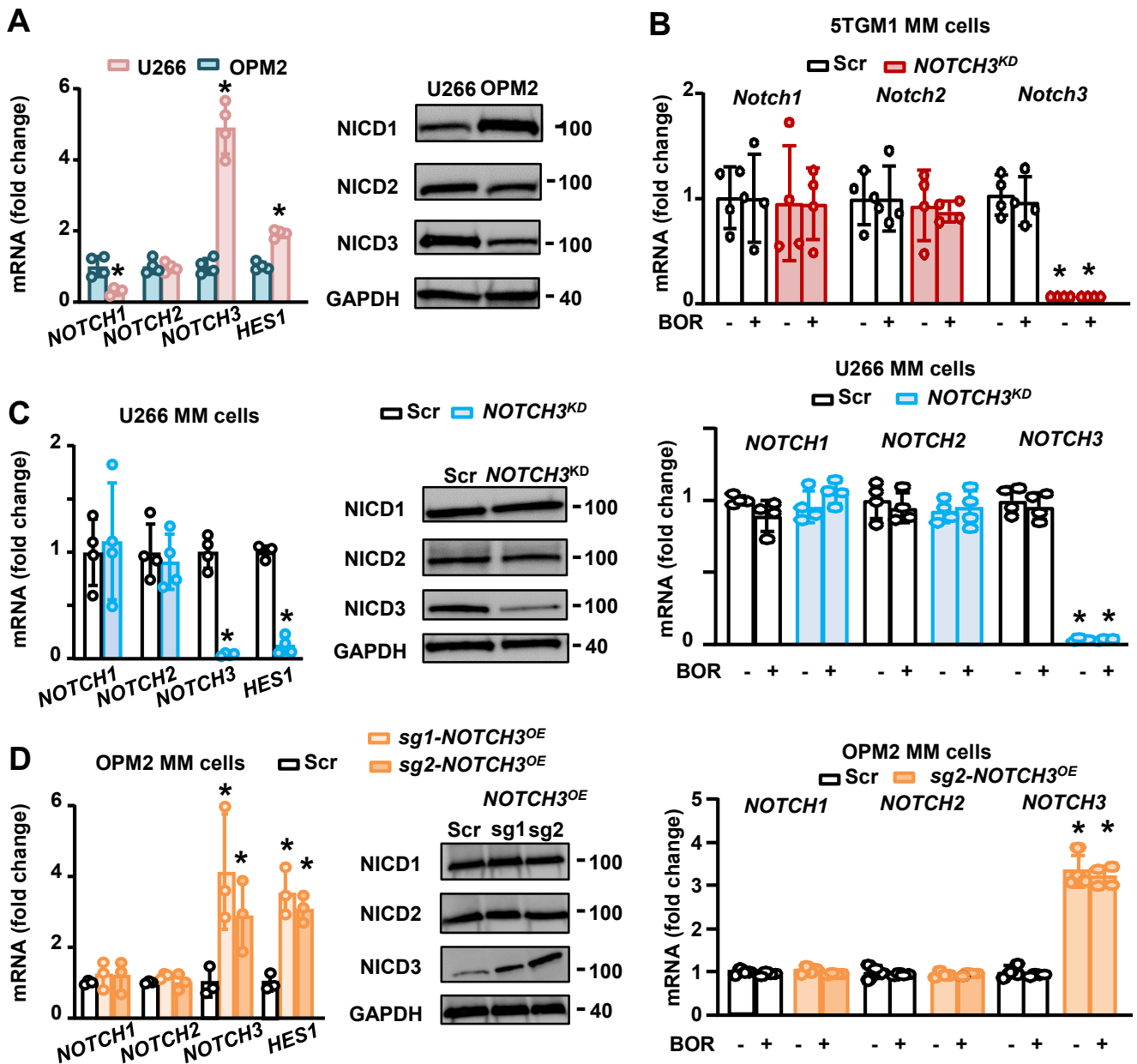
**Supplementary Table 1.** Point mutations in the *NOTCH3* gene detected in newly diagnosed MM patients from the MMRF. N=725 patients. Chr: chromosome; Ref: reference nucleotide; Alt: alteration.



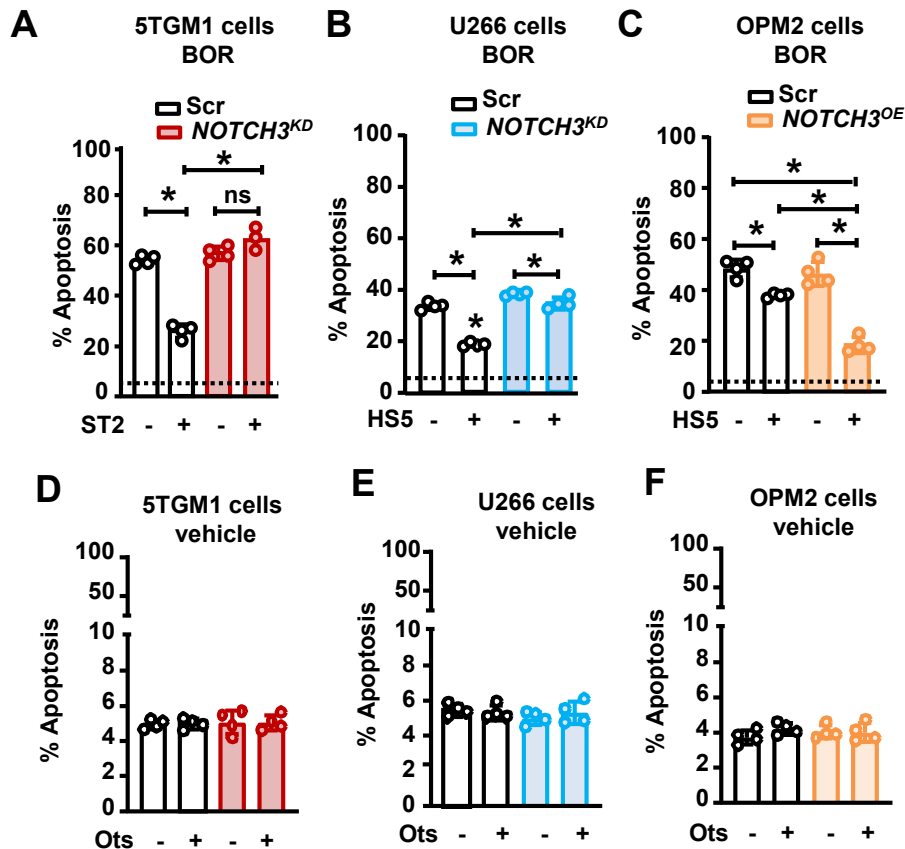
**Supplementary Figure 1. Cells of the TME increase *NOTCH3* expression in MM cell lines.** Gene expression of NOTCH receptors (*NR* 1-4) and the Notch target gene *HES1* in co-cultures of osteocytes (Ots) and (A) murine 5TGM1, (B) human U266, or (C) human OPM2 MM cells after 48h. mRNA expression of (D) murine 5TGM1, (E) human U266, and (F) human OPM2 MM cells cultured in the absence and presence of stromal cells (ST2: murine stromal cells; HS-5: human stromal cells). N=4/group. \* $p < 0.05$  vs. MM cells cultured alone by Student's *t*-test. n.d.: not detected. Data are shown as mean  $\pm$  SD; each dot represents an independent sample. Representative experiments out of two are shown.



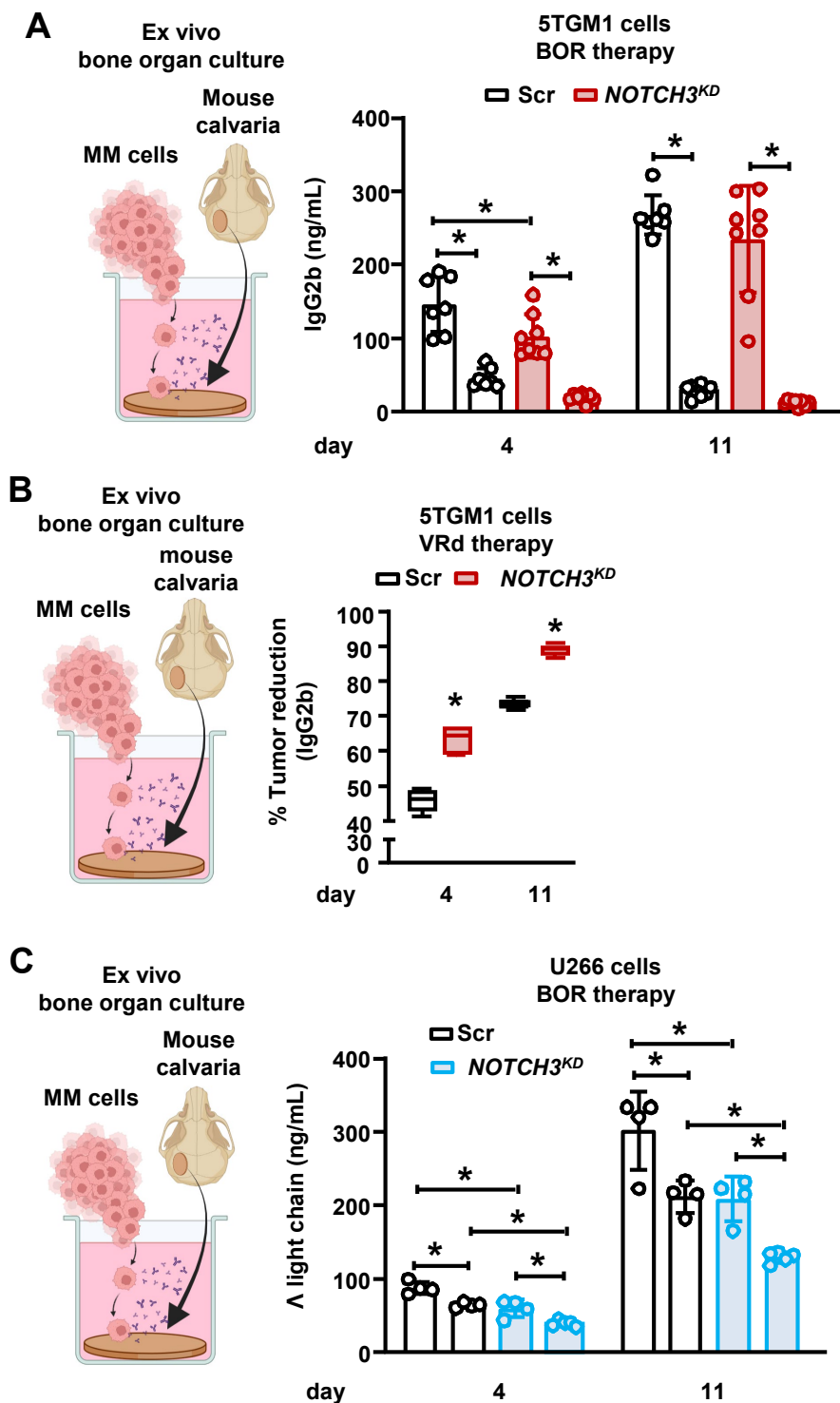
**Supplementary Figure 2. Correlation between *NOTCH1-4* expression and survival in newly diagnosed MM patients.** Kaplan-Meier plots of the overall survival (OS, A) and progression-free survival (PFS, B) of newly diagnosed MM (NDMM) patients with high (blue) vs. low (red) *NOTCH 1-4* expression. (C) Kaplan-Meier plot of the PFS of NDMM patients with high *NOTCH3* expression receiving Bortezomib (BOR)-based therapy (purple line), high *NOTCH3* expression receiving other therapies not including BOR (other; sky blue line), low *NOTCH3* expression receiving BOR-based therapy (green line), low *NOTCH3* expression receiving other therapies not including BOR (other; red line). N=708 patients. Data were analyzed using a Log-rank (Mantel-Cox) test.



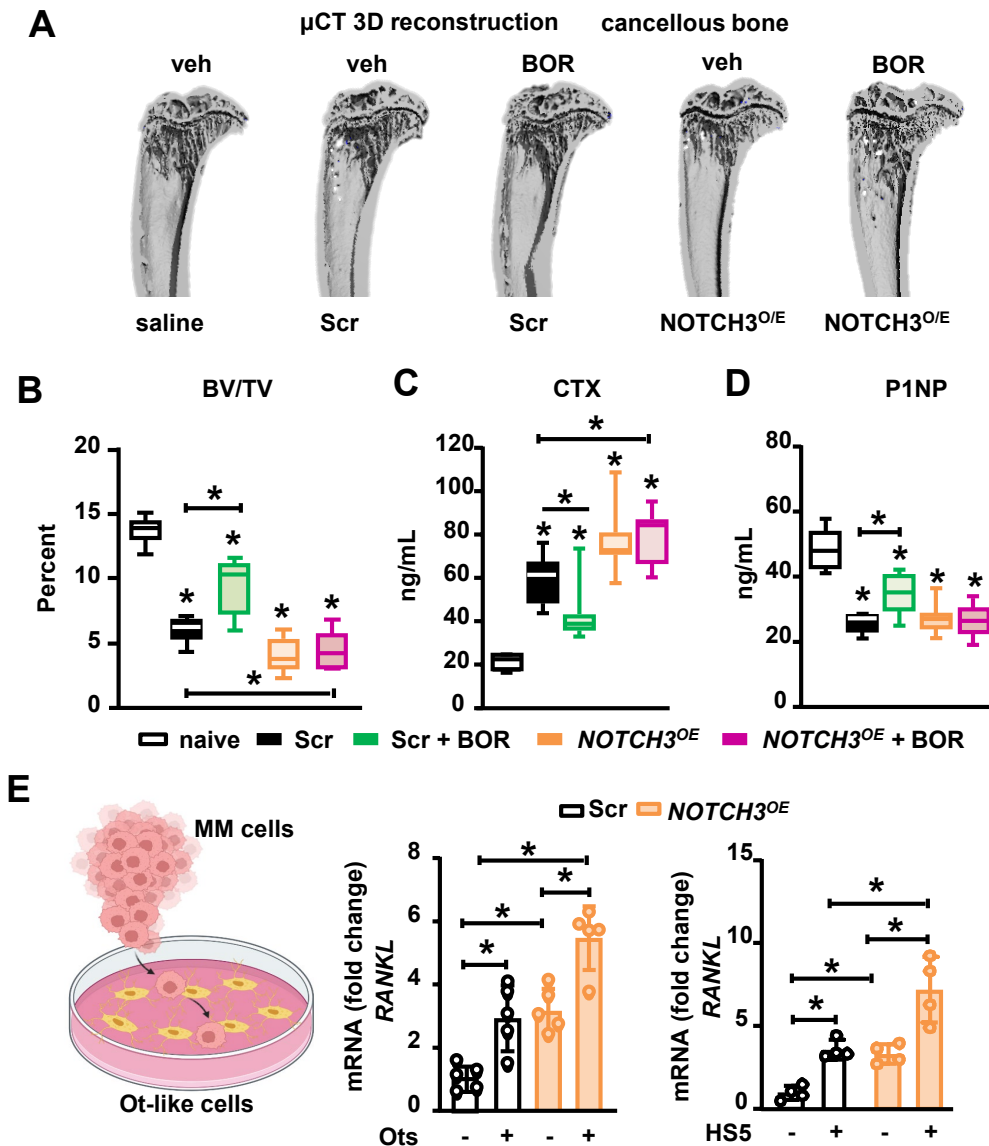
**Supplementary Figure 3. Generation of *NOTCH3* knockdown and activated MM cells.** (A) *NOTCH1-3* receptor expression and cleaved intracellular domain (NICD) protein levels in human U266 and OPM2 MM cells. N=4/group; 48h culture. \* $p < 0.05$  vs OPM2 cells by Student's *t*-test. (B) *NOTCH 1-3* gene expression in scramble (Scr) or genetically modified 5TGM1, U266, and OPM2 MM cells cultured alone and treated with Bortezomib (BOR; 3nM) for 24h. N=4/group; \* $p < 0.05$  vs. scramble MM cells by Two-Way ANOVA, followed by a Tukey post hoc test. *NOTCH 1-3* and *HES1* gene expression and cleaved NICD protein levels in (C) U266 Scr and *NOTCH3* knockdown (*NOTCH3<sup>KD</sup>*) MM cells and (D) OPM2 Scr and *NOTCH3* activated (*NOTCH3<sup>OE</sup>*) MM cells. N=4/group; 48h culture. \* $p < 0.05$  vs. Scr MM cells by Student's *t*-test (C) or One-Way ANOVA, followed by a Tukey post hoc test (D). Data are shown as mean  $\pm$  SD; each dot represents an independent sample. Representative experiments out of two are shown. sg: guide RNA.



**Supplementary Figure 4. NOTCH3 acts as a signaling hub integrating stroma-mediated drug resistance signals.** Percent apoptosis in (A) 5TGM1 scramble (Scr)/*NOTCH3* knockdown (*NOTCH3<sup>KD</sup>*) MM cells, (B) U266 Scr/*NOTCH3<sup>KD</sup>* MM cells, and (C) OPM2 Scr/*NOTCH3* activated (*NOTCH3<sup>OE</sup>*) MM cells cultured in the absence/presence of stromal cells treated with Bortezomib (BOR). Percent apoptosis in (D) 5TGM1 Scr/*NOTCH3<sup>KD</sup>* MM cells, (E) U266 Scr/*NOTCH3<sup>KD</sup>* MM cells, and (F) OPM2 Scr/*NOTCH3<sup>OE</sup>* MM cells cultured in the absence/presence of osteocytes cultured without BOR. N=4/group; BOR=48h. \*p<0.05 by Two-way ANOVA, followed by a Tukey post hoc test. Ots: osteocyte-like cells; ST2: murine stromal cells; HS-5: human stromal cells. Dotted line represents the percent apoptosis in vehicle-treated Scr MM cells cultured alone. ns: non-significant. Data are shown as mean  $\pm$  SD; each dot represents an independent sample. Representative experiments out of two are shown.

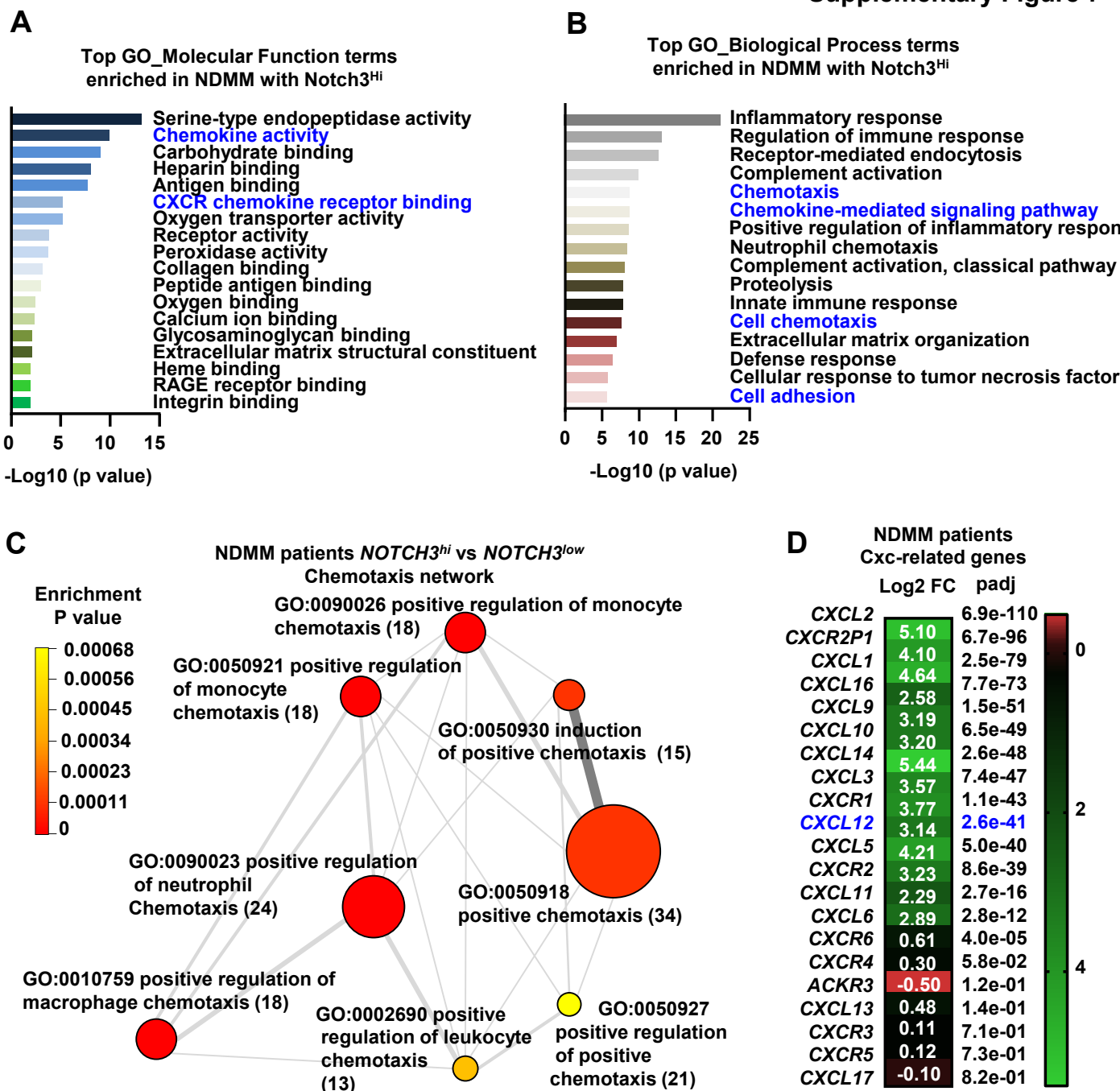


**Supplementary Figure 5. Inhibition of *NOTCH3* sensitizes MM cells to Bortezomib-based treatment.** *Ex vivo* bone-MM organ cultures were established with murine scramble (Scr) and *NOTCH3* knockdown (*NOTCH3<sup>KD</sup>*) 5TGM1 MM cells and calvarial disc bones from C57BL/KaLwRijHsd mice (A, B) or human Scr and *NOTCH3<sup>KD</sup>* U266 MM cells and calvarial disc bones from NSG mice (C). Cultures were treated with Bortezomib (BOR) (A, C) or dexamethasone+BOR+Lenalidomide (VRd) (B) for 4 and 11 days. N=4-8/group. \**p*<0.05 by Two-way ANOVA, followed by a Tukey post hoc test (A, C) or Student's *t*-test (B). Data are shown as mean  $\pm$  SD (A, C); each dot represents an independent sample. Boxes show the data interquartile range, the middle line in the box represents the median, and whiskers the 95% confidence interval of the mean (B).

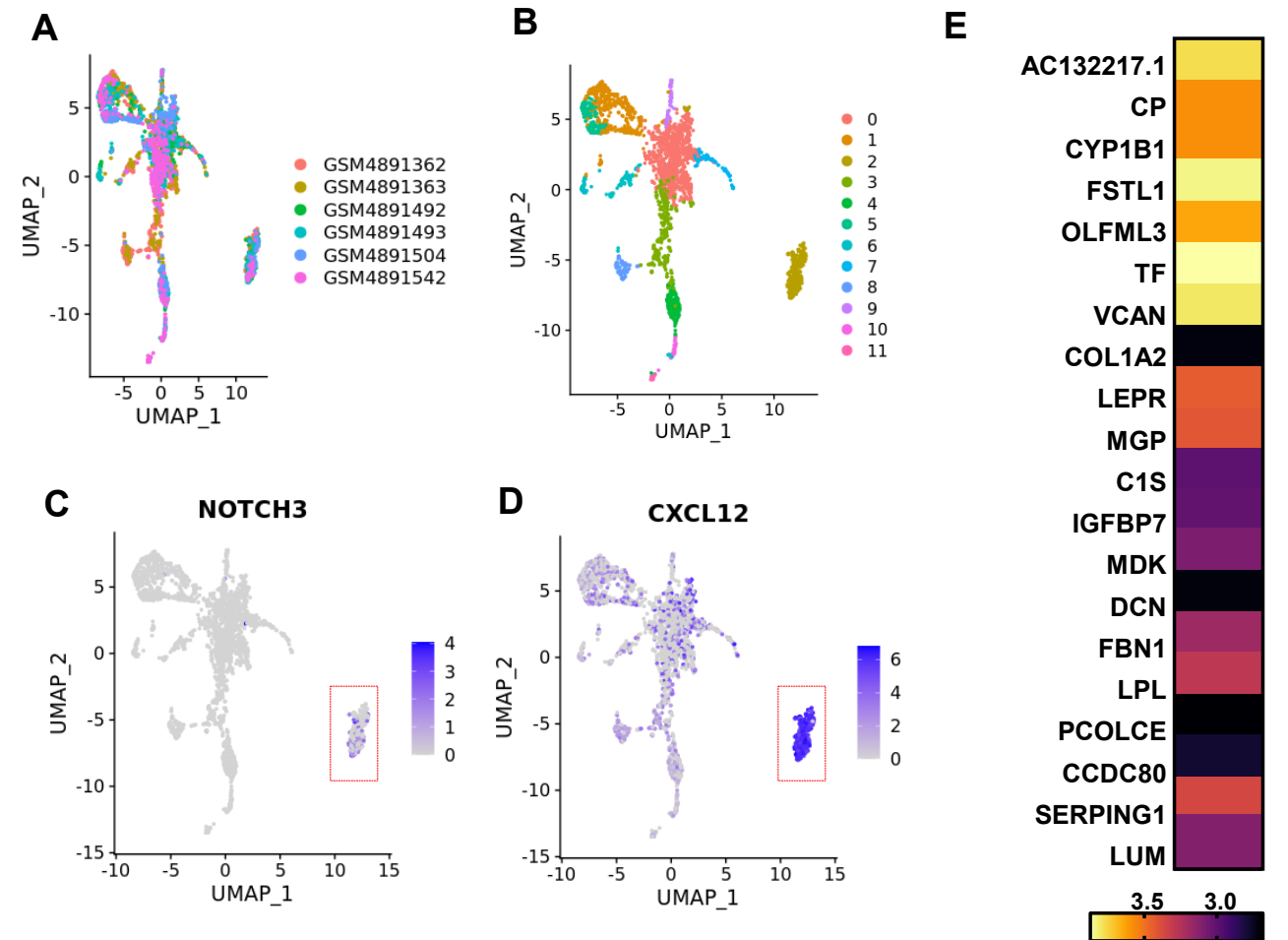


**Supplementary Figure 6. NOTCH3 activation in MM cells impedes the beneficial effects of BOR on bone.** (A) Representative microCT 3D reconstruction images of tibiae, (B) tibiae cancellous bone volume/tissue volume (BV/TV) quantification, serum CTX (C), and P1NP (D) in mice injected with Scramble (Scr) or *NOTCH3* activated (*NOTCH3*<sup>OE</sup>) MM cells and treated with/without Bortezomib (BOR). N=6-11 mice/group. \**p*<0.05 vs. saline by One-way ANOVA, followed by a Tukey post hoc test. Boxes show the data interquartile range, the middle line in the box represents the median, and whiskers the 95% confidence interval of the mean. (B, C, D). (E) *RANKL* gene expression in Scr or *NOTCH3*<sup>OE</sup> MM cells co-cultured with osteocytes (Ots) or stromal cells (HS5). N=4/group. \**p*<0.05 by Two-way ANOVA, followed by a Tukey post hoc test. Representative experiments out of two are shown (E). Data are shown as mean  $\pm$  SD; each dot represents an independent sample (E).





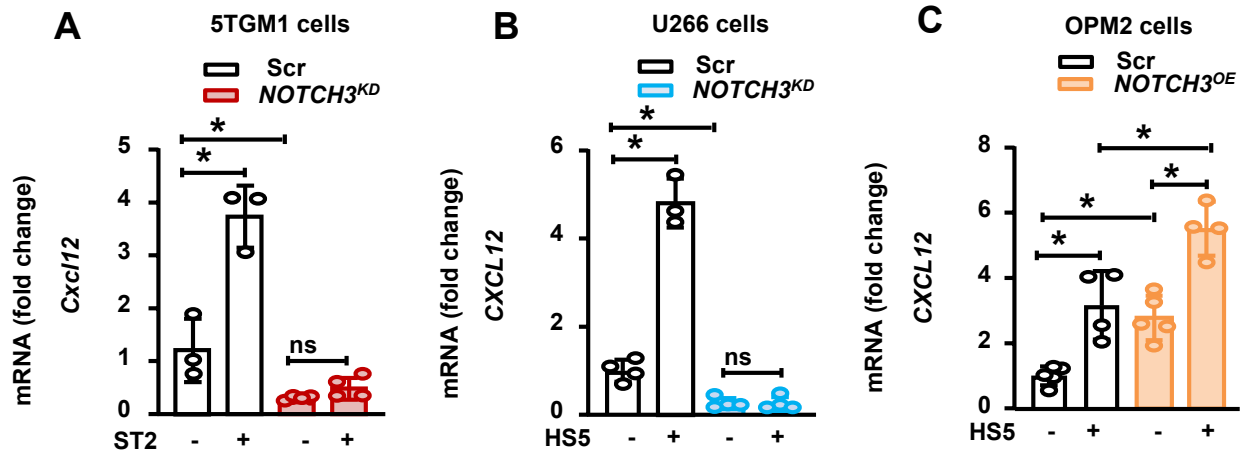
**Supplementary Figure 7. Gene expression and GO term bioinformatics differential analysis in newly diagnosed patients with high vs. low *NOTCH3* expression.** Gene ontology (GO) analysis of upregulated genes in *NOTCH3* high vs. low newly diagnosed MM (NDMM) patients. Bar charts showing the top 20 GO terms for Molecular Function (A) and Biological Process (B) ranked by p-value. N=768 patients. (C) Network plot of selected upregulated functional enrichment analysis of GO terms related to Chemotaxis in NDMM patients with high vs. low *NOTCH3* expression. The size of the circles represents the number of genes in the individual GO terms. N=768 patients. The thickness of the lines represents the number of overlapped genes between the individual GO terms. (D) Differentially expressed CXC-related genes and the corresponding fold changes and adjusted p values in NDMM patients with high vs. low *NOTCH3* expression by Student's t-test. N=768 patients.



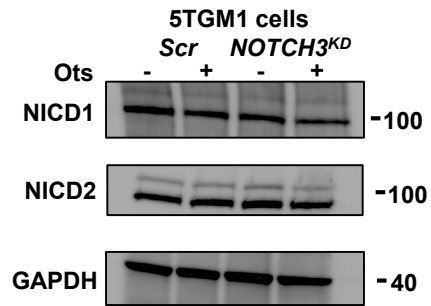
F

GEO_Accession (exp)	Replicate_ID	Sample Name	source_name	SRA Study	Time_point	disease_state	Organ	SAMPLE_TYPE	selection_marker	Cohort
GSM4891362	Kydar04	GSM48913	Bone marrow aspiration	SRP292331	Baseline	PRMM	Bone marrow	Bone marrow aspiration	CD138+/CD38 +	Refractory
		GSM48913	Bone marrow aspiration	SRP292331	Baseline	PRMM	marrow	Bone marrow aspiration	CD138+/CD38 +	Refractory
GSM4891492	Kydar07_Po st2	GSM48914	Bone marrow aspiration	SRP292331	Cycle 10	PRMM	Bone marrow	Bone marrow aspiration	CD138+/CD38 +	
		GSM48914	Bone marrow aspiration	SRP292331	Cycle 10	PRMM	marrow	Bone marrow aspiration	CD138+/CD38 +	
GSM4891504	Kydar29_Po st	GSM48915	Bone marrow aspiration	SRP292331	Cycle 4	PRMM	Bone marrow	Bone marrow aspiration	CD138+/CD38 +	
		GSM48915	Bone marrow aspiration	SRP292331	Cycle 10	PRMM	marrow	Bone marrow aspiration	CD138+/CD38 +	
GSM4891542	Kydar15_Po st2	GSM48915	Bone marrow aspiration	SRP292331	Cycle 10	PRMM	marrow	Bone marrow aspiration	CD138+/CD38 +	

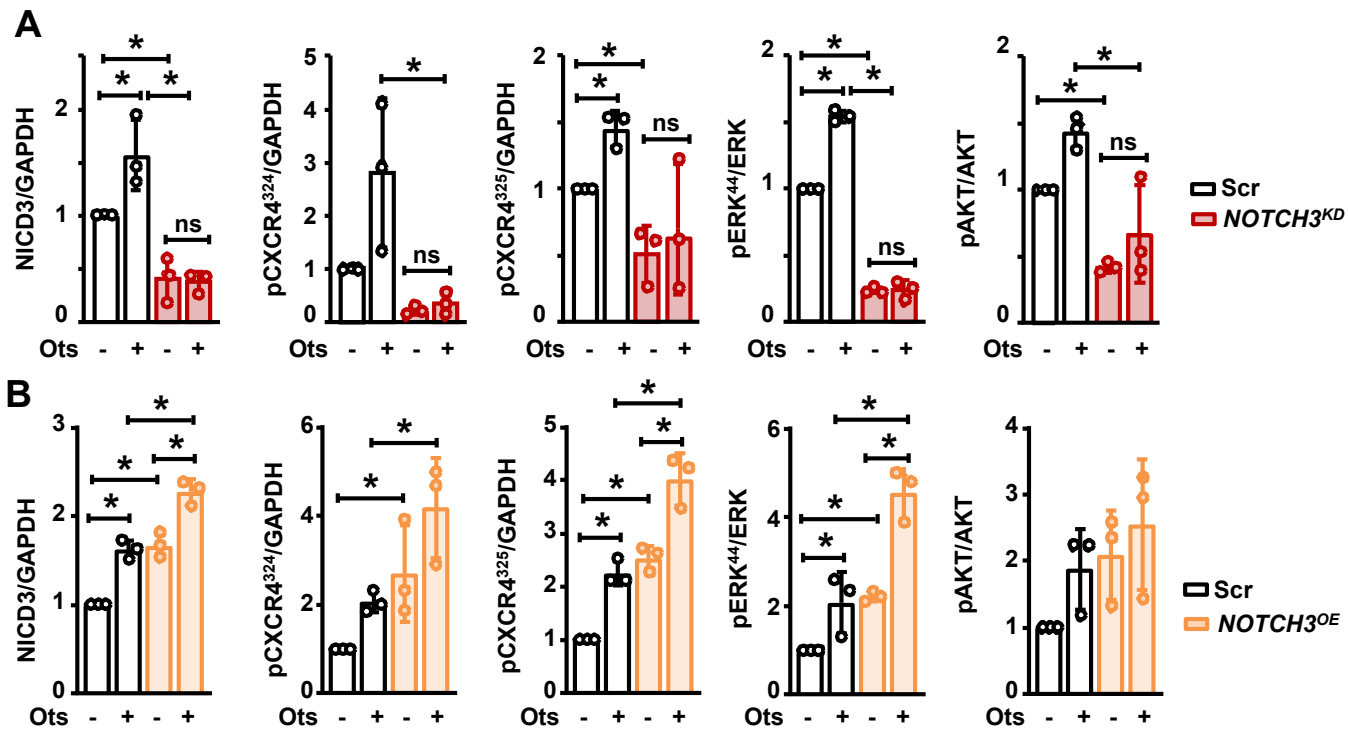
**Supplementary Figure 8. Identification of a population of CD138<sup>+</sup> cells co-expressing *NOTCH3* and *CXCL12* in RRMM patients.** Single-cell RNA-seq analysis, UMAP-based visualization of major classes of CD138<sup>+</sup> cells based on a published single-cell RNA sequencing dataset and colored by patient (A) or cluster (B). Gene expression plot of *NOTCH3* (C) and *CXCL12* (D) of individual CD138<sup>+</sup> cells on UMAP coordinates. (E) Top 20 most upregulated genes in cluster 2 containing *NOTCH3*<sup>+</sup>-*CXCL12*<sup>+</sup> MM cells. (F) Patient and scRNAseq data characteristics.



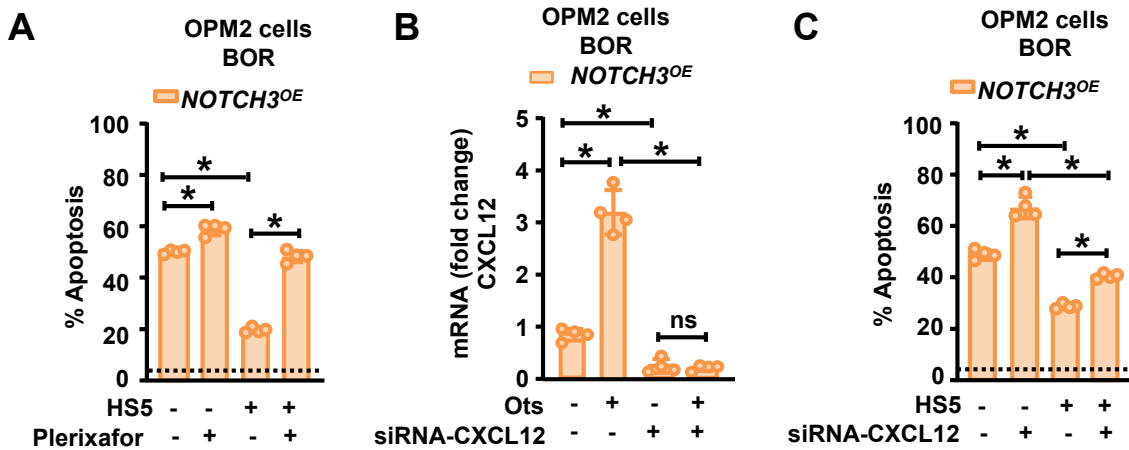
**Supplementary Figure 9. Stromal cell-mediated NOTCH3 signaling regulates *CXCL12* expression in MM cells.** mRNA expression of *CXCL12* in (A) 5TGM1 Scramble (Scr) and *NOTCH3* knockdown (*NOTCH3<sup>KD</sup>*), (B) U266 Scr and *NOTCH3<sup>KD</sup>*, and (C) OPM2 Scr and *NOTCH3* activated (*NOTCH3<sup>OE</sup>*) MM cells cultured for 48h in the absence and presence of stromal cells. ST2: murine stromal cells; HS-5: human stromal cells. N=4/group. \* $p < 0.05$  by Two-way ANOVA, followed by a Tukey post hoc test. ns: non-significant. Data are shown as mean  $\pm$  SD; each dot represents an independent sample. Representative experiments out of two are shown.



**Supplementary Figure 10. Osteocytes do not activate NOTCH1 or NOTCH2 in MM cells.** Cleaved NOTCH1 and 2 intracellular domain (NICD) protein levels in murine Scramble (Scr) or *NOTCH3* knockdown (*NOTCH3<sup>KD</sup>*) 5TGM1 MM cells culture alone or with osteocytes (Ots).



**Supplementary Figure 11. Osteocyte-mediated NOTCH3 signals activate CXCR4 signaling via AKT and ERK phosphorylation.** Quantification of three independent western blots from experiments displayed in Figure 6 A-B using (A) Scramble (Scr) and *NOTCH3* knockdown (*NOTCH3<sup>KD</sup>*) 5TGM1 and (B) Scr and *NOTCH3* activated (*NOTCH3<sup>OE</sup>*) OPM2 MM cells co-cultured in the absence/presence of osteocytes (Ots). N=3/group. \* $p < 0.05$  Two-Way ANOVA, followed by a Tukey post hoc test. Data are shown as mean  $\pm$  SD; each dot represents an independent sample.



**Supplementary Figure 12. Genetic or pharmacologic inhibition of CXCL12 signaling prevents stroma-mediated drug resistance to Bortezomib-based therapies.** (A) Percent apoptosis in *NOTCH3* activated (*NOTCH3<sup>OE</sup>*) OPM2 MM cells treated with Bortezomib (BOR) in the presence/absence of Plerixafor and cultured with/without osteocytes (Ots). N=4/group; BOR=48h. \* $p < 0.05$  by Two-Way ANOVA, followed by a Tukey post hoc test. (B) *CXCL12* gene expression in *NOTCH3<sup>OE</sup>* OPM2 MM cells treated with/without siRNAs against *CXCL12* and cultured alone or with Ots. N=4; \* $p < 0.05$  by Two-way ANOVA, followed by a Tukey post hoc test. (C) Percent apoptosis in *NOTCH3<sup>OE</sup>* OPM2 MM cells treated with BOR in the presence/absence of *siRNA-CXCL12* and cultured with/without Ots. N=4/group; BOR=48h. \* $p < 0.05$  by Two-Way ANOVA, followed by a Tukey post hoc test. Data are shown as mean  $\pm$  SD; each dot represents an independent sample. Dotted line represents the percent apoptosis in vehicle-treated OPM2 MM cells cultured alone. siRNA: small interference RNA. Representative experiments out of two are shown.

## Supplementary methods.

**Reagents.** RPMI 1640 media, Minimum Essential Media (MEM)  $\alpha$ , fetal bovine serum, bovine calf serum, Normocin, antibiotics (penicillin/streptomycin), TriZol, and DiI/DiD cell trackers were purchased from Invitrogen Life Technologies (Grand Island, NY, USA). Trypan Blue was purchased from Sigma Aldrich (St. Louis, MO, USA).  $\gamma$ -secretase inhibitor XX (GSI-XX) was purchased from Calbiochem (San Diego, CA, USA). Anti-GAPDH (Cat#2118S, RRID: AB\_561053), anti-NOTCH1 (Cat #4380S, RRID: AB\_10691684), anti-NOTCH2 (Cat #5732S, RRID: AB\_10693319), anti-p-ERK (Cat#9101, RRID: AB\_331646), anti-ERK (Cat#9102, RRID: AB\_330744), anti-pAKT (Cat# 4060S), and anti-AKT (Cat# 9272S) antibodies were purchased from Cell Signaling Technologies (Danvers, MA, USA); anti-NOTCH3 (ab23426, RRID: AB\_776841), anti-NOTCH4 (ab166605), and anti-pCXCR4 (ab74012, RRID: AB\_1523429) antibodies were purchased from Abcam (Cambridge, MA, USA). Plerixafor (Cat#S8030), Bortezomib (Cat#S1013), and Lenalidomide (Cat#S1029) were purchased from Selleckchem (Houston, TX, USA); Dexamethasone (Cat#D4902) was purchased from Sigma (St. Louis, MO, USA); and *CXCL12* siRNA (Cat#SR304303) was purchased from Origene Technology (Rockville, MD, USA). Puromycin (Cat#58-58-2) and Blastidicin (Cat#ant-bl) were purchased from InvivoGen (San Diego, CA, USA).

**Cell culture.** 5TGM1 murine MM cells (RRID: CVCL\_VI66) were obtained from Dr. B. Oyajobi (University of Texas at San Antonio, TX, USA), and MLO-A5 murine osteocyte-like cells (RRID: CVCL\_0P24) were purchased from Kerafast (Boston, MA, USA). OPM2 (RRID: CVCL\_1625) and U266 (RRID: CVCL\_0566) human MM cells were obtained from Dr. G. D. Roodman (Indiana University, IN, USA). ST2 murine stromal cells (RRID: CVCL\_2205) were obtained from Dr. Jin-Ran Chen (University of Arkansas for Medical Sciences, AR, USA), and HS-5 human stromal

cells (RRID: CVCL\_3720) were purchased from ATCC (Manassas, VA, USA). Cell lines were checked for mycoplasma weekly and routinely examined for proper morphology, population doubling, and paraprotein production. MM cell lines (5TGM1, OPM2, U266) were cultured in RPMI with 10% FCS and 1% P/S. Osteocyte-like cells (MLOA5) were cultured on calf skin collagen type I-coated plates in  $\alpha$ MEM media with 2.5% FBS, 2.5% BCS, and 1% P/S. Stromal cells (ST2, HS5) were cultured in DMEM with 10% FBS and 1% P/S.

**Gene Expression.** Total RNA was isolated from MM cells and bone tissues using Trizol and converted to cDNA (Invitrogen Life Technologies), following the manufacturer's directions. EDTA incubations were used to separate MM cells from the osteocytes/stroma, as previously described.<sup>1,2</sup> Gene expression was quantified by quantitative real-time PCR (qPCR) using TaqMan assays from Applied Biosystems (Foster City, CA, USA), following the manufacturer's directions. Gene expression levels were calculated using the comparative threshold (CT) method and were normalized to the housekeeping gene GAPDH.<sup>1,2</sup>

**Western Blot.** Cell lysates (50 $\mu$ g) were boiled in the presence of SDS sample buffer (NuPAGE LDS sample buffer; Invitrogen) for 10 minutes and subjected to electrophoresis on 10% SDS-PAGE (Bio-Rad Laboratories). Proteins were transferred to PVDF membranes using a semidry blotter (Bio-Rad) and incubated in a blocking solution (5% nonfat dry milk in TBS containing 0.1% Tween-20) for 1 hour to reduce nonspecific binding. Immunoblots were performed using anti-GAPDH, pCXCL12, AKT, pAKT, ERK, pERK, NOTCH1, NOTCH2, and NOTCH3 antibodies (1:1000) followed by goat anti-rabbit secondary antibodies, conjugated to horseradish peroxidase (1:2000) in 5% milk (Santa Cruz Biotechnology). Western blots were developed using an enhanced chemiluminescence detection assay following the manufacturer's directions (Bio-Rad). Protein bands were quantified using ImageJ.



**Enzyme-linked immunoassays (ELISA).** The levels of the tumor biomarkers human lambda (Bethyl Laboratories; Cat#E88-116) or IgG2B (Invitrogen; Cat#88-50430-88) paraproteins produced by OPM2/U266 and 5TGM1 cells, respectively, were used to determine tumor growth/burden *in vivo* (serum) and *ex vivo* (conditioned media). The bone resorption biomarker C-telopeptide of type 1 collagen (CTX) (Immunodiagnostic systems; Cat#AC-06F1) and bone formation marker propeptide of type 1 collagen (P1NP) (Immunodiagnostic systems; Cat#AC-33F1) were analyzed in serum (*in vivo*). Tumor growth/burden, bone resorption, and bone formation were determined using commercially available specific ELISA and following the manufacturer's recommendations.

**Apoptosis and proliferation assays.** Apoptosis in MM cells was assessed by flow cytometry using the FITC (OPM2 or U266) or PerCP-Cyanine5.5 (5TGM1) Annexin V apoptosis Detection kit (BD Biosciences) following the manufacturer's recommendations. For analysis of apoptosis in co-cultures, OPM2 cells were selected by using mCherry fluorescence, and 5TGM1 and U266 cells were stained with the fluorescent cell-tracker DiD before plating cells (emission 665 nm; excitation 645 nm) following the manufacturer's recommendations. Samples were analyzed in a BD FACSCalibur (UAMS Core Facility for Flow cytometry) within 1h. At least 10,000 cells were used for each group, and the data were analyzed by FlowJo software to detect different cell populations. Co-cultures were treated with Plerixafor (25uM), BOR (3nM), VRd (BOR: 2nM, Lenalidomide: 1uM, Dexamethasone: 10nM) were refreshed every 24h. OPM2 cells were stained with a fluorescent cell tracker DiI before plating cells following the manufacturer's recommendations for proliferation analysis. After 48h of culture, cells were collected, re-suspended in PBS, and DiI fluorescence was read at 520 to 565 nM on a plate reader.

**Genetic inhibition/activation in MM cells.** Control and *NOTCH3* knockdown 5TGM1 MM cells were generated as described before.<sup>2</sup> To generate stable control and *NOTCH3*-activated OPM2 MM cells, we first transduced cells with CRISPRa dCas9-VP64 lentiviral particles (MOI=10; Addgene, Watertown, MA, USA) and treated them with Blasticidin (5ug/mL) for selection. OPM2 MM cells stably expressing CRISPRa dCas9-VP64 were transduced with lentiviral particles carrying scramble or *NOTCH3* directed sgRNAs (TCCGCGCGTCCCAGGCTGTG) and mCherry (MOI=10; Genecopoeia, Rockville, MD. USA) and treated with Puromycin (1ug/mL) for selection. To generate control and *NOTCH3* knockdown U266 MM cells, cells were transduced with a plasmid containing a sgRNA sequence against *NOTCH3* cloned into a guide RNA Cas9 vector (a gift from Dr. Helena Karlström, Karolinska Institutet, Sweden)<sup>3</sup> and treated with Puromycin (3ug/mL) for selection. 5TGM1 transduced MM cells were maintained in complete media supplemented with 3ug/mL of Puromycin, OPM2 cells were maintained in complete media supplemented with 0.5ug/mL Puromycin and 2.5 µg/mL Blasticidin, and U266 cells were maintained in complete media supplemented with 1.5ug/mL Puromycin. To transiently inhibit CXCL12 in MM cells, we treated OPM2 MM cells with 1.0 nM of siRNA against CXCL12 for 24h before establishing MM-osteocyte/stroma co-cultures.

**Ex vivo organ cultures.** Ex vivo MM-murine bone organ cultures were established with calvarial bones from NOD.Cg-Prkdcscid Il2rgtm1 Wjl/SzJ (NSG; Jackson's Lab, strain: 005557) for human U266 or OPM2 MM cells or with calvarial bones from C57BL/KaLwRijHsd mice of murine 5TGM1 MM cells, as described before.<sup>1</sup> For these ex vivo cultures,  $5 \times 10^4$  MM cells were plated on calvarial bones, and  $2 \times 10^5$  MM cells were plated on human bones. The human bone samples were obtained from 2 males, with no pathologies or medications that could affect bone mass or architecture. Treatments (Plerixafor 50uM; BT-GSI 10 uM; BOR 3nM; VRd: BOR 2nM,

Lenilidomide 1 $\mu$ M, Dexamethasone 10nM) were refreshed every 3 days. 50% of conditioned media was collected and replaced after 4 days of culture. All conditioned media was collected after 11 days of culture. Tumor growth was quantified by luciferase activity or ELISA.

**Bioinformatic analyses.** We segregated high vs. low *NOTCH3* patients using quartile measures and performed comparative gene expression analysis as described before.<sup>2</sup> The gene list for the GSEA on responses to BOR was constructed using data from Mulligan et al.<sup>4</sup> Samples were classified as progressive/relapsed if they met two criteria: i) the patient must have a baseline sample, and ii) the patient must have a sample taken after either a complete or partial response. The scRNASeq analysis was conducted on data previously published by Cohen et al. (GSE161195).<sup>5</sup> Salmon gene count data were imported into and normalized using the R package DESeq2. Differential expression analysis of *NOTCH3* high versus low samples was performed using DESeq2, with an adjusted p-value cutoff of 0.05. Gene set enrichment analysis was then conducted using the R package fgsea.<sup>6</sup> Survival analyses were performed and visualized in R using the survival and survminer packages. Comparison of gene expression between NDMM (n=768) and paired NDMM vs. progression/relapsed (PRMM; n=70) samples was performed and visualized using the R package ggpubr. Correlation analysis between *CXCL12* and *NOTCH3* was performed in both the NDMM and progressive/relapsed samples using the R package ggpubr. Mutation data for *NOTCH3* was obtained from the MMRF Researcher Gateway for corresponding whole-exome sequencing samples (n=725). All single-cell analyses were performed using the R package Seurat as described before.<sup>7</sup> The PIANO package was used to perform the gene-set enrichment analysis of Gene Ontology (GO) and gene networks using adjusted p-value and log<sub>2</sub> fold changes as the input to calculate the enrichment p-value of the GO terms.<sup>8</sup> For human cell line mutation analysis, the (HMCL69\_Preliminary\_Mutations\_Samtools.xlsx) file was utilized to

determine which cell lines were mutated for NOTCH3, which was downloaded from the Keats Lab repository (<https://www.keatslab.org>).

## References

1. Delgado-Calle J, Anderson J, Cregor MD, et al. Bidirectional Notch Signaling and Osteocyte-Derived Factors in the Bone Marrow Microenvironment Promote Tumor Cell Proliferation and Bone Destruction in Multiple Myeloma. *Cancer Res.* 2016;76(5):1089-1100.
2. Sabol HM, Amorim T, Ashby C, et al. Notch3 signaling between myeloma cells and osteocytes in the tumor niche promotes tumor growth and bone destruction. *Neoplasia.* 2022;28(10):785.
3. Wu D, Wang S, Oliveira DV, et al. The infantile myofibromatosis NOTCH3 L1519P mutation leads to hyperactivated ligand-independent Notch signaling and increased PDGFRB expression. *Dis Model Mech.* 2021;14(2):
4. Mulligan G, Mitsiades C, Bryant B, et al. Gene expression profiling and correlation with outcome in clinical trials of the proteasome inhibitor bortezomib. *Blood.* 2007;109(8):3177-3188.
5. Cohen YC, Zada M, Wang SY, et al. Identification of resistance pathways and therapeutic targets in relapsed multiple myeloma patients through single-cell sequencing. *Nat Med.* 2021;27(3):491-503.
6. Korotkevich G, Sukhov V, Budin N, Shpak B, Artyomov MN, Sergushichev A. Fast gene set enrichment analysis. *bioRxiv.* 2021;060012.
7. Satija R, Farrell JA, Gennert D, Schier AF, Regev A. Spatial reconstruction of single-cell gene expression data. *Nat Biotechnol.* 2015;33(5):495-502.

8. Patro R, Duggal G, Love MI, Irizarry RA, Kingsford C. Salmon provides fast and bias-aware quantification of transcript expression. *Nat Methods*. 2017;14(4):417-419.

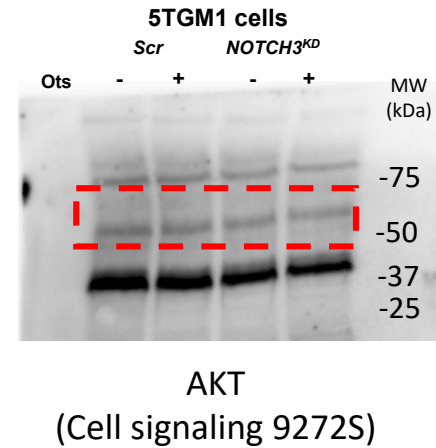
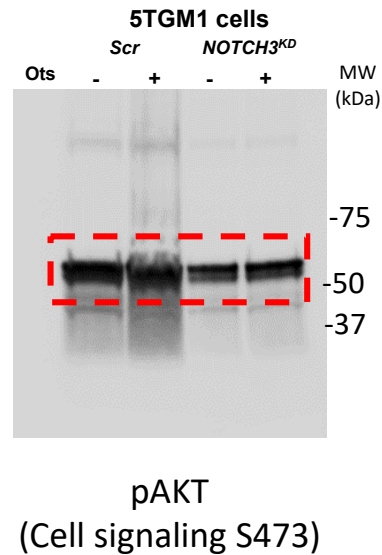
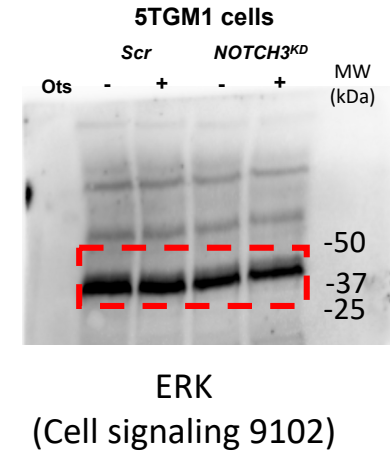
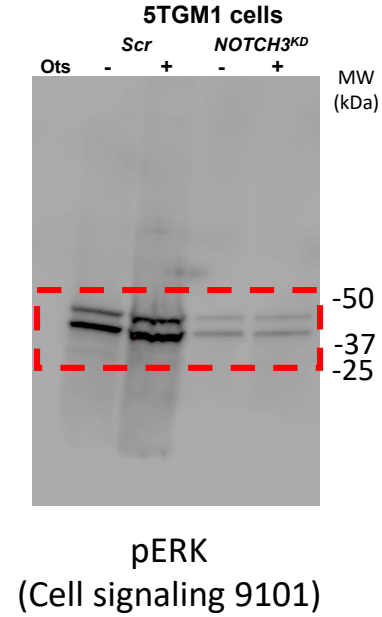
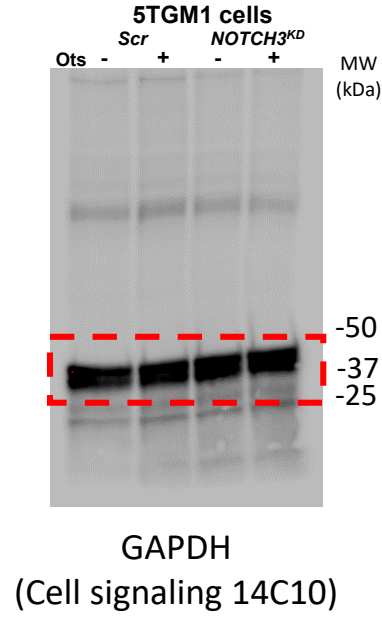
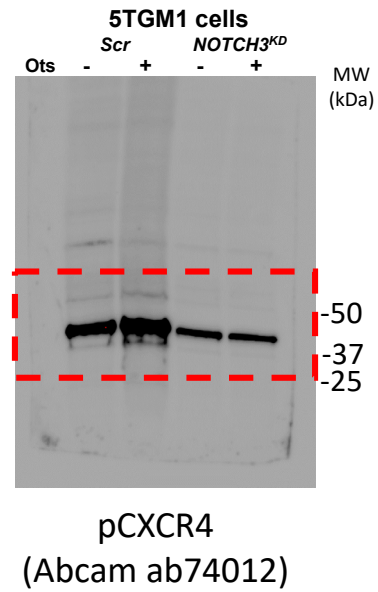
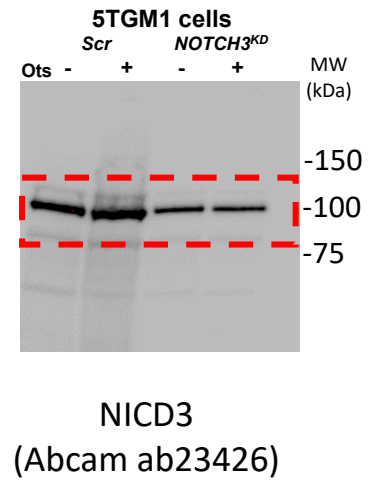
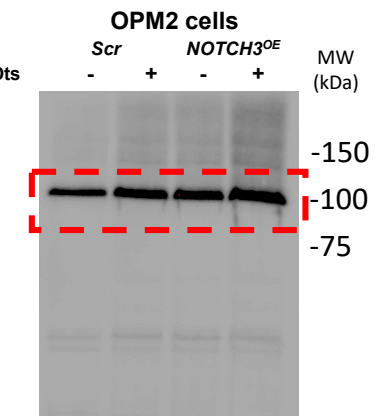
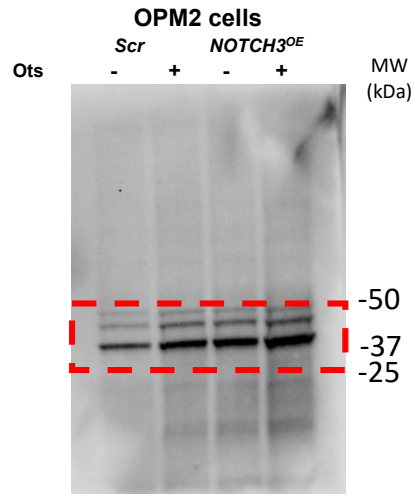


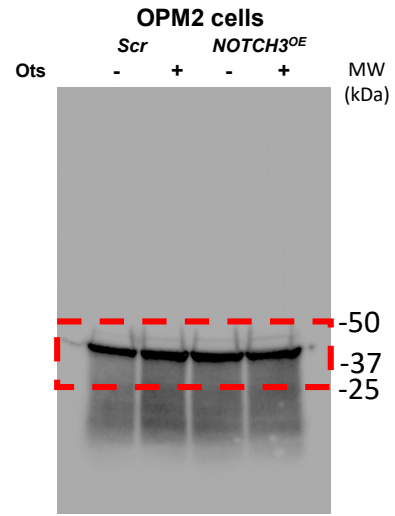
Figure 6A



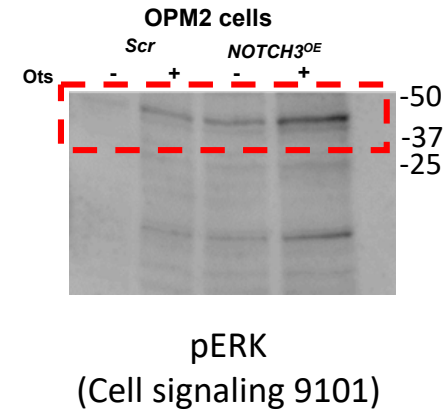
NICD3  
(Abcam ab23426)



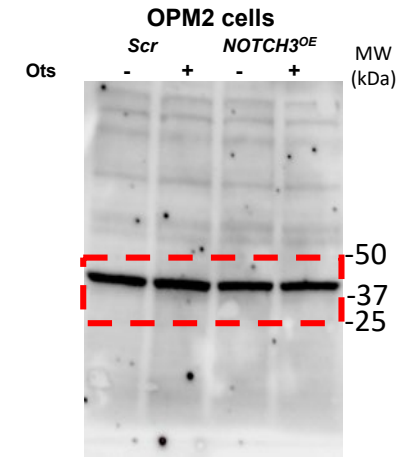
pCXCR4  
(Abcam ab74012)



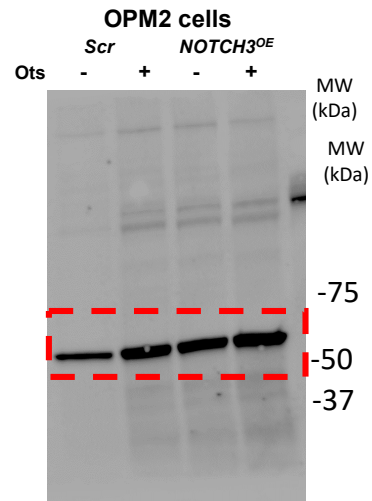
GAPDH  
(Cell signaling 14C10)



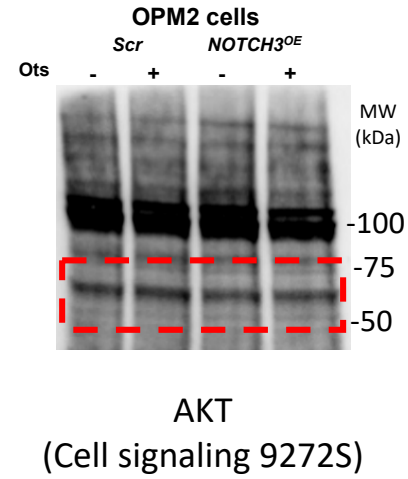
pERK  
(Cell signaling 9101)



ERK  
(Cell signaling 9102)

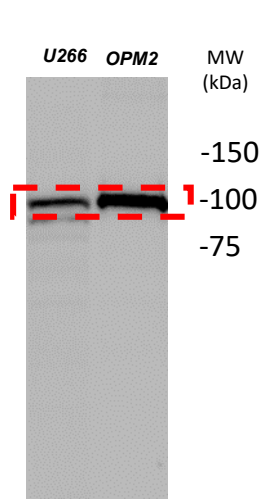


pAKT  
(Cell signaling S473)

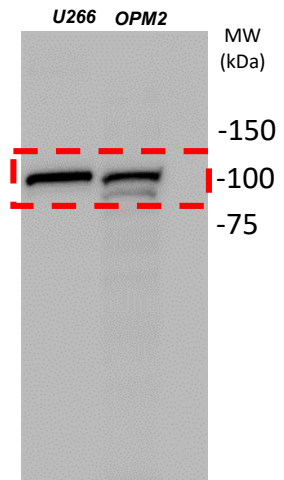


AKT  
(Cell signaling 9272S)

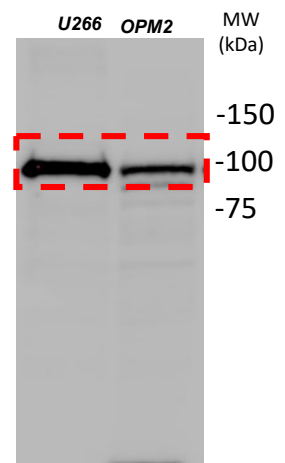
Figure 6B



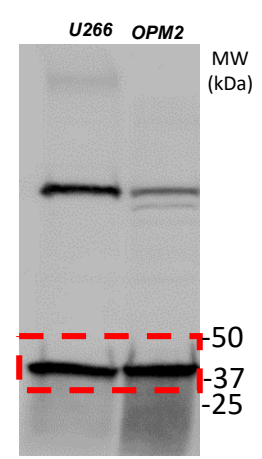
Notch1  
(Cell signaling D6F11)



Notch2  
(Cell signaling D76A6)

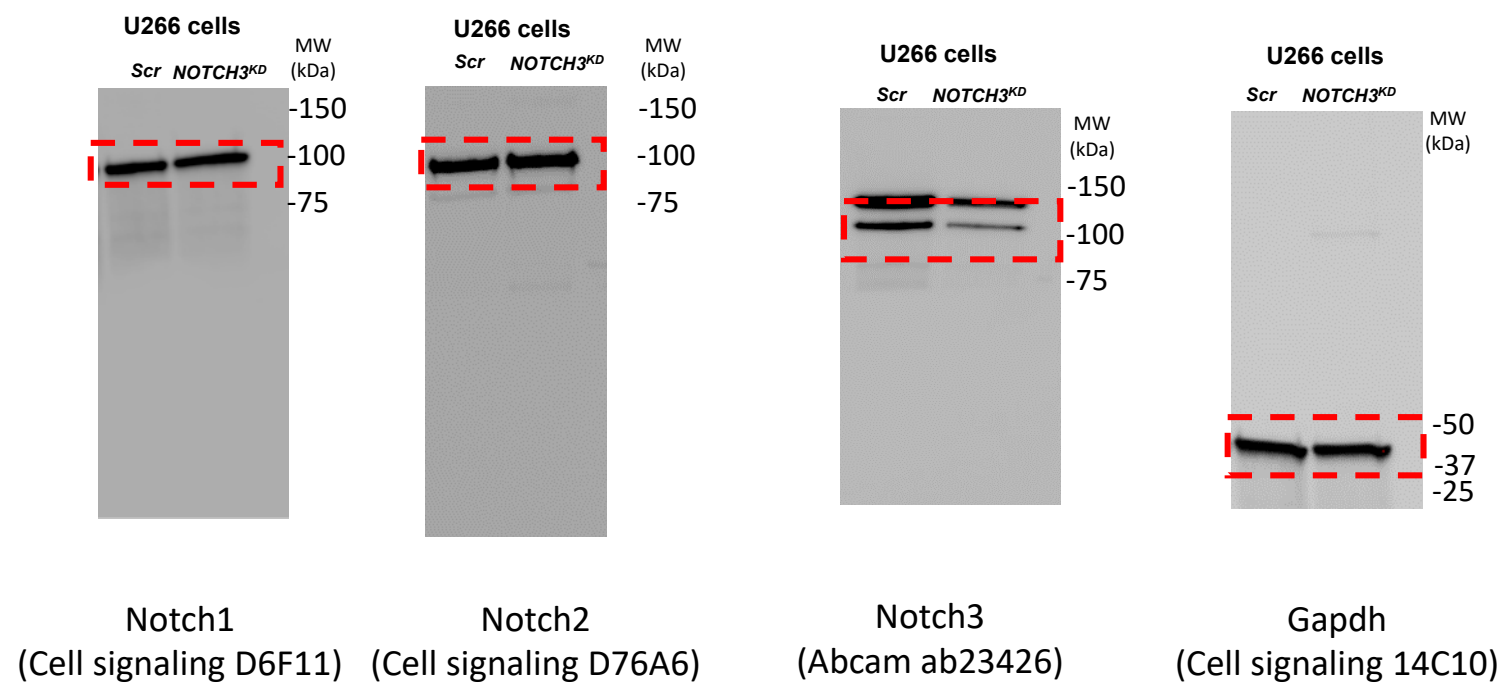


Notch3  
(Abcam ab23426)

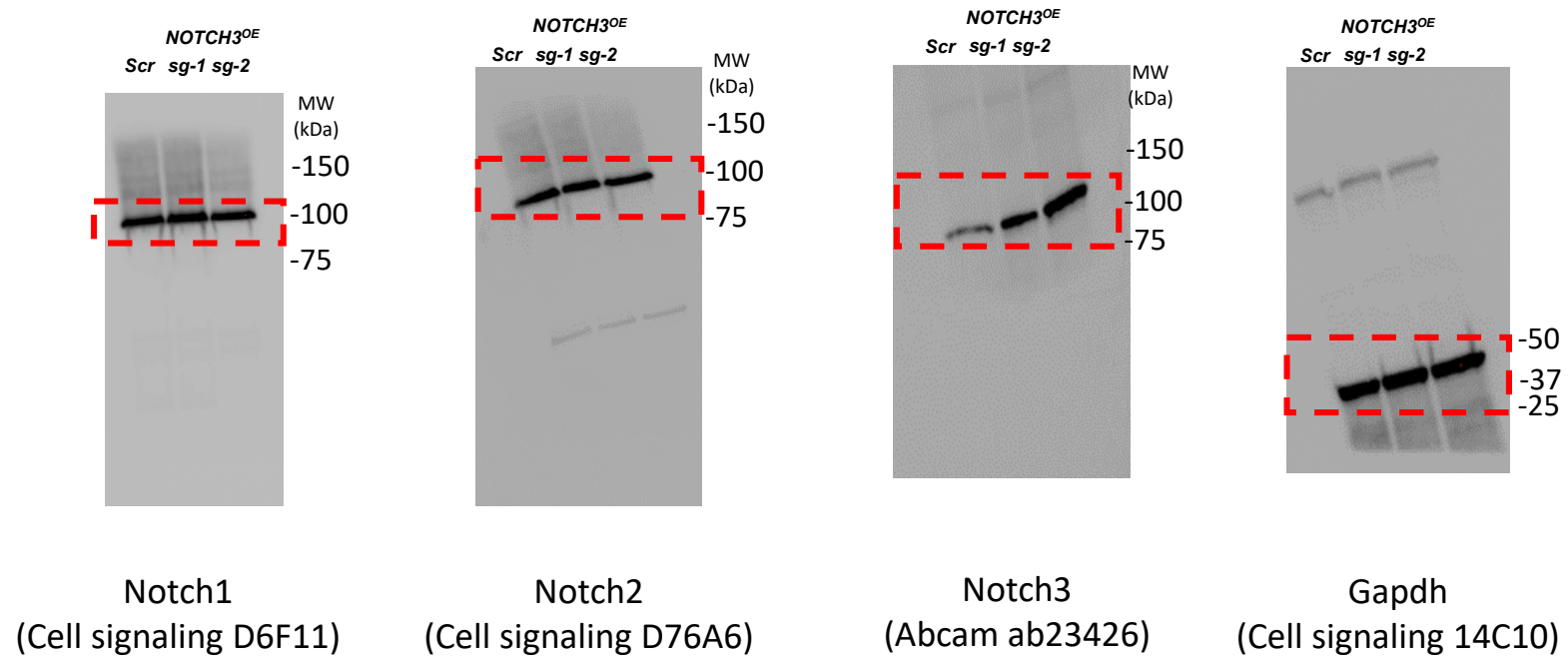


Gapdh  
(Cell signaling 14C10)

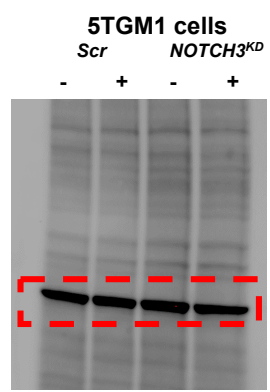




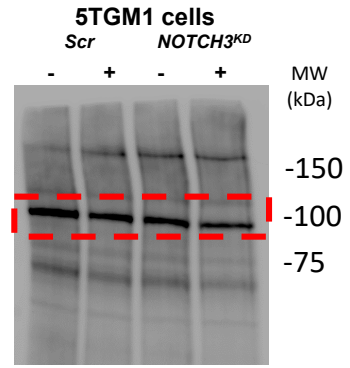
Supp. Fig 3b



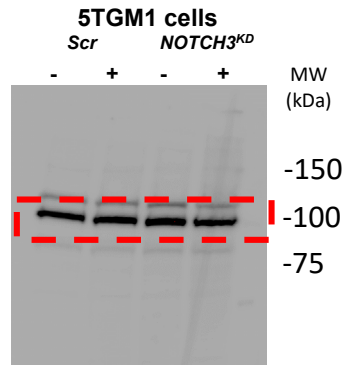
Supp. Fig 3c



Gapdh  
(Cell signaling 14C10)



Notch1  
(Cell signaling D6F11)



Notch2  
(Cell signaling D76A6)